A Study on Static Image Derived Input Function for Non-invasively Constructing Parametric Image in Functional Imaging

Xian Shi, Lingfeng Wen, Weidong Cai, David Dagan Feng
Biomedical and Multimedia Information Technology (BMIT) Research Group,
School of Information Technologies, University of Sydney,
Sydney, Australia

Lingfeng Wen,
Department of PET and Nuclear Medicine,
Royal Prince Alfred Hospital,
Sydney, Australia

David Dagan Feng
Centre for Multimedia Signal Processing (CMSP),
Department of Electronic & Information Engineering, Hong Kong Polytechnic University,
Hong Kong, China

Abstract— **Positron emission tomography (PET), as functional imaging, provides in-vivo spatial distribution of physiological or biochemical processes. The kinetic modelling process to derive quantitative functional parameter usually requires invasive frequent blood sampling. We proposed a new approach to use static imaging derived information to produce non-invasive input function (SID-IF). The performance of SID-IF was investigated by 609 clinical neurological studies in non-invasively constructing parametric images of cerebral metabolic rate of glucose consumption (CMRGlc). The performance of the personal information feature based input function method (PIFB-IF) was also evaluated in the investigation. The results of area under curve and CMRGlc demonstrated the image feature derived by cerebellum provided less bias in the estimation of SID-IF. The performance of SID-IF was sensitive to the choice of the training set and the plasma glucose concentration in the data set may improve the estimated accuracy. The PIFB-IF method was less sensitive to the glucose range and choice of training set.**

Keywords: Functional imaging, Positron Emission Tomography, Kinetic modelling, Non-invasive method.

I. INTRODUCTION

Medical imaging is an important component in modern medicine through computerized imaging techniques to visualize detailed anatomical or functional information in human body for disease diagnosis and treatment assessment. Positron emission tomography (PET), as functional imaging, provides *in-vivo* spatial distribution of physiological or biochemical processes [1, 2]. One of the unique benefits of functional imaging is its ability in detecting subtle functional changes at early stage of disorder without marked changes detectable in anatomical imaging, such as computed tomography (CT) and magnetic resonance imaging (MRI).

With the kinetic modelling technique, PET imaging can derive parametric image, which depicts quantitative functional parameters in three dimensions and facilitates objective evaluation in the diagnosis. Kinetic modelling, assuming an underlying kinetic model for a given tracer, usually requires a plasma time activity curve (PTAC) as an input function (IF) and a tissue time activity curve (TTAC) as the output function. For example, FDG (*[^{18}F] 2-fluorodeoxy-glucose*), the popular tracer for glucose metabolism, has a three-compartment and four-parameter compartment model. The procedure of invasive frequent blood sampling for deriving PTAC not only leads to discomfort to patients, and also gives rises to radiation and potential infection to clinical staff.

Efforts have been paid to address the challenge in frequent invasive blood sampling. One approach is to rely on dynamic images and use TTACs for blood pools, such as carotid or aorta, as the image derived input function (ID-IF) [3-5]. The reference tissue model [6-8] is another approach applied in neuroreceptor study when a reference tissue is available for describing non-specific binding of neuroreceptor. However, the dynamic imaging is impractical to be applied in a busy clinical centre due to the required prolonged scanning time.

For static imaging in clinical routine, the population based input function (PB-IF) [9, 10] is an alternative approach, assuming that the shape of IF is similar to derive individual IF from a population-based standardized IF with a few blood samples as calibration. Arterialized-venous blood sampling has been also reported in the calibration of the PB-IF [11]. Without any blood samples, another approach was proposed to use the scale factor derived from patient's body weight, body height and injected dose to calibrate one corrected standardized IF as a personal information feature based method (PIFB-IF) [10, 12].

This work was supported in part by ARC and PolyU grants.

In this study, we proposed a new approach to use static imaging derived information to estimate non-invasive input function. The method was referred to as SID-IF. The performance of proposed method was evaluated by 609 clinical neurological studies of FDG-PET in non-invasively constructing parametric image of glucose metabolism. Meanwhile, we also investigated the performance of PIFB-IF for our clinical data.

II. MATERIALS AND METHODS

A. Clinical Data

There were 609 patients (322 males, 287 females) included in this investigation. All the patients were referred to have neurological FDG-PET studies for brain tumour (282 patients) or epilepsy (327 patients) studies from 2003 to 2009 in the Department of PET and Nuclear Medicine, Royal Prince Alfred Hospital (Camperdown, NSW, Australia). Across the subjects, the mean age was 39.5 ± 15.5 (y), the mean body height was 170.3 ± 11.0 (cm), the mean body weight was 74.7±17.5 (kg), the mean body mass index (BMI = body weight/(body height)^2) was 25.7 ± 5.4 (kg/m^2) and 340.0 ± 32.0 MBq FDG was injected for each patient.

Approximate 7-minute static scans were performed on a Siemens Biograph 2 PET-CT scanner after a 52.0 ± 6.5 min uptake time. Two arterialized-venous blood samples (post-injection 10 min and 45 min) were taken to derive the mean scale factor (SF) to derive a population-based input function as the calibration [11]. The obtained IF was referred to as the true IF in this paper. The plasma glucose concentration of subjects was 84.1 ± 12.9 (mg/dL).

B. SID-IF Method

The proposed SID-IF method consists of two components. The first is to apply spatial normalization to define volume of interest (VOI) for brain cortex; the second is to use the VOI based mean value as the feature in a linear equation for deriving the scale factor to calibrate the population-based input function.

1) Spatial normalisation

To reduce operator's subjective bias in delineating region of interest, the SPM2 package (Wellcome Trust centre for neuroimaging, London, U.K.) was used in automatic spatial normalization for the obtained uptake images of patients. The patient image volume with the dimensions of 128 × 128 × 47 and a voxel size of 1.840 × 1.840 × 3.375 mm^3 were spatially normalized to a PET brain template with the dimensions of 91 × 109 × 91 voxels with a voxel size of 2 × 2 × 2 mm^3. The MNI-based Tzourio-Mazoyer atlas was then used to define VOI [13].

2) Linear equation for scale factor

We are assuming there is a correlation between static images derived features and the scale factor for calibrating population-based IF. In this paper, a linear relationship was investigated by the linear least squares fitting technique for the given equation in equation (1),

$$y = ax + b \tag{1}$$

where x is a value derived from static image according to labelled atlas [13], and y is true scale factor derived by two arterialized-venous blood samples. Four different inputs of x were investigated, including the mean value of whole cortex, the mean value of cerebellum, and the mean value of cerebellum normalized by body weight and BMI. The SID-IF was then estimated as following:

$$Cp_{i.SID-IF}(t) = y_i \times SIF(t) \tag{2}$$

where $SIF\ (t)$ is the standard input function and y is estimated scale factor derived from equation (1) from the static image based values.

C. PIFB-IF Method

The PIFB-IF method was assuming the injected dose distributed by an estimated distribution volume (EDV) and the ratio between the injected dose and EDV was proportional to the initial distribution volume of FDG [10]. The EDV was derived according to equation (3),

$$EDV = c \times H^a \times W^b \tag{3}$$

where H is body height, W is body weight, a, b are independent variables generated with minimum coefficient of variation (CV) of an assumed constant across subjects, and c is another variable generated from a, b and initial input function. Then a PIFB-IF corrected standard input function (SIF_{cor}) could be derived by using mean of EDV and net inject dose of training data [10] and an individual IF based on PIFB-IF method could be calibrated as following:

$$Cp_{i.PIFB-IF}(t) = \left(\frac{NID_i}{EDV_i} \right) \times SIF_{\text{cor}}(t) \tag{4}$$

D. Evaluation

The whole dataset was randomly divided to 2 groups for training and evaluation. 304 subjects were chosen for training of the linear equation for scale factor and 305 subjects were chosen as the validation group.

The area under the curve (AUC), the time integral of the input function, was used in the evaluation. The AUC was calculated using a simple trapezoid algorithm. The percentage error of AUC was calculated between the estimated and the original IF:

$$\%\text{error of } AUC = \left| \frac{AUC_{\text{est}} - AUC_{real}}{AUC_{real}} \right| \times 100\% \tag{5}$$

where AUC_{real} is the AUC obtained from the true IF and the AUC_{est} obtained from the estimated IF.

The performance of the SID-IF and PIFB-IF was further evaluated by constructing the parametric images of cerebral metabolic rate of glucose consumption (CMRGlc) by the autoradiography method [10] according to equation (6),

$$CMRGLc = \frac{Cg}{LC} \bullet \frac{C_t(T) - \frac{k_1}{\alpha_2 - \alpha_2}[(k_4 - \alpha_1)e^{-\alpha_1 t} + (\alpha_2 - k_4)e^{-\alpha_2 t}] \otimes C_p(t)}{\frac{k_2 + k_3}{\alpha_2 - \alpha_1}(e^{-\alpha_1 t} - e^{-\alpha_2 t}) \otimes C_p(t)}$$

$$\alpha_{1,2} = \sqrt{k_2 + k_3 + k_4 \mp \sqrt{(k_2 + k_3 + k_4)^2 - 4k_2 k_4}} \quad (6)$$

where Cg is the plasma glucose concentration (in mg/dL), LC is the lumped constant, equal to 0.418 describing the relationship between glucose and FDG metabolism, $C_t(T)$ is the decay-corrected radioactivity concentration in the brain at time T (middle time of static imaging frame), and $\otimes$ denotes the mathematic convolution, $C_p(t)$ is the IF; k_1, k_2, k_3, and k_4 are the mean rate constants of FDG kinetic model for human brain cortex: $k_1 = 0.102$ ml·min^{-1}·ml^{-1}, $k_2 = 0.13$ min^{-1}, $k_3 = 0.062$ min^{-1}, $k_4 = 0.0068$ min^{-1}.

The obtained CMRGlc images were then spatially normalized by SPM2. The error percentage of CMRGlc was derived according to the following equation:

$$\%error \text{ of } CMRGLc = \left| \frac{CMRGLc_{\text{est}} - CMRGLc_{real}}{CMRGLc_{real}} \right| \times 100\% \quad (7)$$

where $CMRGlc_{real}$ is the CMRGlc obtained from the true input function and $CMRGlc_{est}$ is the CMRGlc obtained from the estimated input function. The VOI definitions in the MNI atlas were used to define VOI for whole brain cortex, cerebellum, temporal cortex, parietal cortex, occipital cortex and frontal cortex.

Because plasma glucose concentration affects glucose metabolism in human body, it may affect blood clearance in IF and the estimated accuracy of SID-IF and CMRGlc. By taking the glucose distribution of whole dataset (Figure. 1) into account, we further divided the whole dataset into four smaller groups with specific plasma glucose concentration: 70-100 (mg/dL), 75-95 (mg/dL), 85-95 (mg/dL). Each group of subset data was further randomly divided into two groups respectively for training and evaluation. The estimated biases of AUC of SID-IF were derived according to equation (5).

The performances of SID-IF and PIFB-IF may be dependent on the given training set. Thus, ten sets of randomly generated training set and evaluation set were used in the assessment of the reliability of the investigated methods.

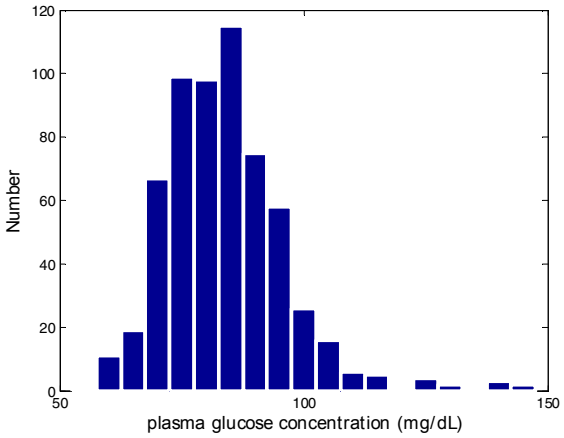

Figure 1. The distribution of plasma glucose concentration across 609 FDG-PET neurological studies

III. RESULT

A. Parameters for SID-IF and PIFB-IF

The formula for EDV generated by our clinical data was (a, b, c) = (0.64, 0.47, 49.16) for the PIFB-IF method (r=0.494).

The parameter set (a, b) of the linear equation for scale factor in the SID-IF method was (0.61, 1.20) for the mean cortex (r=0.170), (0.83, 1.08) for the mean cerebellum (r=0.227), (31.24, 1.35) for the mean cerebellum normalized by body weight (r=0.201), (0.00, 1.33) for the mean cerebellum normalized by BMI (r=0.190).

B. Percentage Error of AUC

Table I lists the percentage error of AUC of the PIFB-IF and the SID-IF with four different image-derived inputs as well as the four subsets of plasmas glucose concentration.

In the first group, the full range of dataset with the plasma glucose concentration ranging from 50 to 150 mg/dL, the SID-IF with the mean cerebellum normalized by body weight achieved the least bias of AUC, which was 12.5±10.6%. It is obvious that the SID-IF using the mean cerebellum value was better than the SID-IF using the cortex mean value.

TABLE I. THE PERCENTAGE ERROR OF AUC FOR THE INVESTIGATED METHODS (MEAN ± STANDARD DEVIATION %)

Glucose range (mg/dL)	[50,150]	[70,100]	[75,95]	[85,95]
Number of training Data set	304	245	187	87
Number of test data set	305	245	187	87
SID-IF: Mean of cortex	13.3±10.8 (r=0.240)	12.8±10.5(r=0.270)	12.4±9.5(r=0.308)	11.0±8.6(r=0.398)
SID-IF: Mean of cerebellum	12.7±10.6 (r=0.283)	12.3±10.1(r=0.314)	11.6±9.2(r=0.374)	10.4±8.0(r=0.458)
SID-IF: Mean of cerebellum/weight	12.5±10.6(r=0.302)	12.4±10.5(r=0.306)	11.8±9.8(r=0.377)	10.8±8.5(r=0.454)
SID-IF: Mean of cerebellum/BMI	12.7±10.4(r=0.297)	12.3±10.2(r=0.321)	11.7±9.5(r=0.360)	11.3±8.5(r=0.391)
PIFB-IF method	11.0±10.6(r=0.356)	11.0±10.5(r=0.351)	10.4±10.0(r=0.445)	11.1±9.5(r=0.334)

TABLE II. PERCENTAGE ERROR OF CMRGLC FOR THE SUBSET GROUP WITH THE GLUCOSE CONCENTRATION RANGING FROM 85~95 MG/DL (MEAN ± STANDARD DEVIATION %)

	Whole Cortex	Cerebellum	Temporal cortex	Parietal cortex	Occipital cortex	Frontal cortex
SID-IF: Mean of cortex	14.1±12.2	14.2±12.4	14.3±12.5	14.0±12.1	14.0±12.2	13.8±12.0
SID-IF: Mean of cerebellum	14.2±14.0	14.2±13.5	14.5±14.9	14.1±13.7	14.2±14.7	14.0±14.1
SID-IF: Mean of cerebellum/weight	14.6±13.1	14.6±12.5	14.9±14.0	14.5±13.0	14.6±13.9	14.4±13.3
SID-IF: Mean of cerebellum/BMI	15.1±14.0	15.1±13.6	15.4±14.9	15.0±13.6	15.2±14.8	14.9±14.1
PIFB-IF method	14.6±12.9	14.7±13.1	14.8±13.2	14.5±12.8	14.5±12.8	14.3±12.5

However, percentage error of AUC of all the SID-IF methods are slightly worse than the PIFB-IF method. It is interesting to observe that errors of AUC of the SID-IF methods were decreasing while the range of glucose concentration was narrower.

Table II lists the mean values of CMRGlc for the VOIs for the same data with the range of plasma glucose concentration being 85 to 95 in Table I. The similar accuracy of CMRGlc was observed as compared with the biases achieved by the SID-IF and PIFB-IF.

Fig. 2 plots one example of the true IF and the estimated SID-IF. Fig. 3 plots the corresponding CMRGlc images for the true IF (a) and the estimated SID-IF (b).

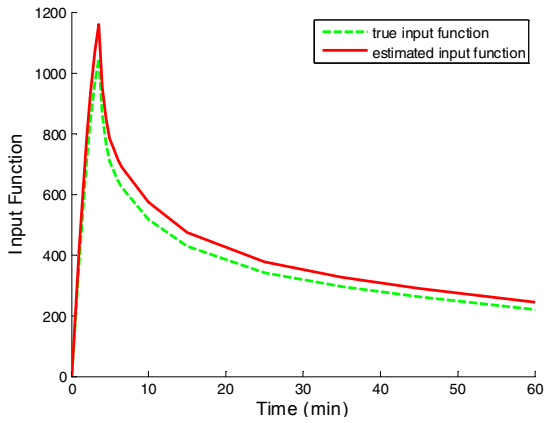

Figure 2. True IF and estimated SID-IF

C. *Effect of Traning Sets*

Table III lists the mean and relevant standard deviation of percentage error of AUC for the ten times of randomly sampled training sets. The results demonstrated that the accuracy of SID-IF was dependent on the choice of training set, while PIFB-IF was relatively insensitive to the choice of training set.

Fig. 4 plots the changes of the percentage bias of AUC for the two investigated methods. Similar bias and trends of AUC were observed between the SID-IF and PIFB-IF for the data with the glucose concentration range of [85, 95] as shown in Fig. 4 (b). However, for other range of glucose concentration investigated, slightly higher biases were achieved by the SID-IF as shown in Fig. 4 (a).

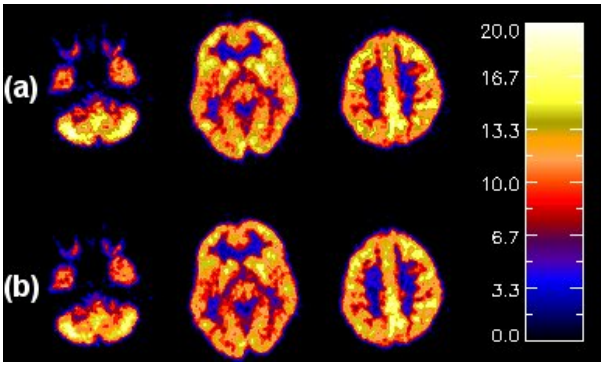

Figure 3. CMRGLc images (a) true IF; (b) SID-IF

IV. DISCUSSION AND CONCLUSION

Fig. 5 plots the reduction of percentage bias of AUC of SID-IF and PIFB-IF as compared with the full data set according to equation (8):

$$\%\ error\ reduction = \left| \frac{\%error\ of\ AUC_{group} - \%error\ of\ AUC_{full}}{\%error\ of\ AUC_{full}} \right| \times 100\% \quad (8)$$

Evident trend was observed that the error of AUC was decreasing as the range of plasma glucose concentration was narrower. This implies that glucose concentration would affect the accuracy of estimated IF derived by SID-IF. On the contrary, the estimated biases of PIFB-IF method were not sensitive to glucose changes.

TABLE III. MEAN PERCENTAGE ERROR OF AUC OF TEN RANDOMLY SAMPLED EXPERIMENTS

Glucose range (mg/dL)	[50,150]	[70,100]	[75,95]	[85,95]
Number of training Data set	304	245	187	87
Number of test data set	305	245	187	87
SID-IF: Mean of cortex	14.8±14.6	13.8±12.5	13.4±11.4	11.8±8.6
SID-IF: Mean of cerebellum	14.2±14.1	13.3±12.1	12.8±11.1	11.2±8.2
SID-IF: Mean of cerebellum/weight	13.9±15.9	13.2±14.7	12.7±12.4	11.5±10.1
SID-IF: Mean of cerebellum/BMI	14.2±15.7	13.3±14.5	12.7±11.9	11.7±9.5
PIFB-IF method	11.8±12.9	11.3±11.0	11.1±10.4	11.2±9.3

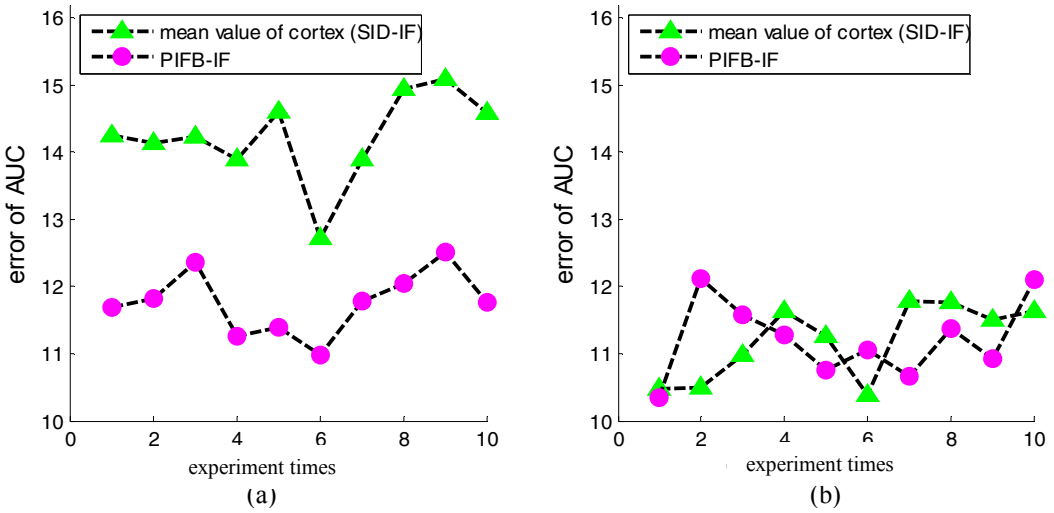

Figure 4. True Plots of percentage bias of AUC for SID-IF and PIFB-IF methods as a function of random experiment times. (a) Glucose range of 50 to 150 (mg/dL); (b) glucose range of 85-95 (mg/dL)

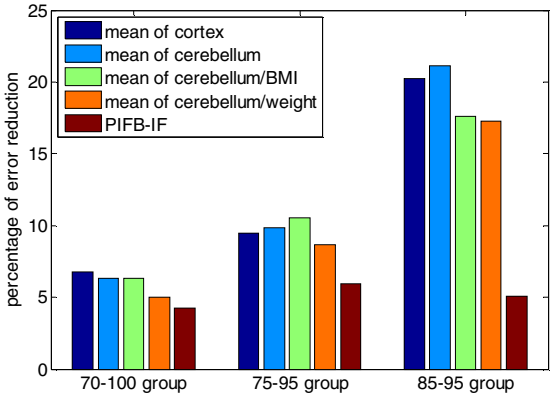

Figure 5. Percentage error reductions of 3 groups

The current error analysis of AUC and CMRGLc may be dependent on the random choice of training and evaluation data. Statistical evaluation methods, such as the ten-fold cross-validation would be applied in the future investigation.

This paper proposed a new static image derived input function method. The results of AUC and CMRGlc demonstrated the image feature derived by cerebellum provided less bias in the estimation. The performance of the static image derived feature method was sensitive to the choice of the training set, while the plasma glucose concentration in the data set may improve the estimated accuracy. On the contrary, the patient information feature based method was less sensitive to the glucose range and the choice of training set.

REFERENCES

[1] F.Yuhua, K.Tsair, L.Renshyan, and W.Liangchih, "Estimating the input function non-invasively for FDG-PET quantification with multiple linear regression analysis: simulation and verification with in vivo data," European Journal of Nuclear Medicine and Molecular Imaging, vol. 31, 2004, pp. 692-702

[2] T. Ahmed, et al., "Noninvasive in vivo measurement of vascular inflammation with F-18 fluorodeoxyglucose positron emission tomography," Journal of Nuclear Cardiology, vol. 12, 2005, pp. 294-301.

[3] J. Mourik, "Image-derived input functions for PET brain studies", European Journal of Nuclear Medicine and Molecular Imaging, vol. 36, 2009, pp. 463-471.

[4] Z.F. Paolo, et al., "Comparison of eight methods for the estimation of the image-derived input function in dynamic ^{18}F-FDG PET human brain studies," Journal of Cerebral Blood Flow & Metabolism, vol. 29, 2009, pp. 1825-1835.

[5] G. Hongbin, A.R. Rosemary, C. Kewei, "An input function estimation method for FDG-PET human brain studies", Nuclear Medicine and Biology, vol. 34, 2007, pp. 483-492.

[6] R. N. Roger, A. L. Adriaan, P. H. Susan and J. C. Vincent, "Parametric imaging of ligand-receptor binding in PET using a simplified reference region," Neuroimage, vol. 6, 1997, pp. 279.

[7] Z. Yun, et al., "An extended simplified reference tissue model for the quantification of dynamic PET with amphetamine challenge," Neuroimage, vol.33, 2006, pp. 550-563.

[8] A. A. Lammertsma and P. H. Susan, "Simplified Reference Tissue Model for PET Receptor Studies," Neuroimage, vol. 4, 1996, pp. 153-158

[9] W. Kazuo, et al., "Simplification for measuring input function of FDG PET: Investigation of 1-point blood sampling method", The Journal of Nuclear Medicine, vol. 41, 2000, pp. 1484.

[10] S. Toshiki, et al., "Noninvasive estimation of FDG input function for quantification of cerebral metabolic rate of glucose: optimization and multicenter evaluation," Journal of nuclear medicine, vol. 41, 2000, pp. 1612-1618.

[11] S. Eberl, A.R. Anayat, R.R. Fulton, P.K. Hooper, M.J. Fulham, "Evaluation of two population-based input functions for quantitative neurological FDG PET studies," European Journal of Nuclear Medicine, vol. 24, 1997, pp. 299-304.

[12] T. Tsuchida, et al., "Noninvasive measurement of cerebral metabolic rate of glucose using standardized input function," The Journal of Nuclear Medicine, vol. 40, 1999, pp. 1441.

[13] N. Tzourio-Mazoyer, et al., "Automated anatomical labeling of activations in SPM using a macroscopic anatomical parcellation of the MNI MRI single-subject brain," Neuroimage, vol. 15, 2002, pp. 273-289.